Extended abstract

High entropy alloys for fusion applications

André Ruza

andre.ruza@tecnico.ulisboa.pt

Abstract

In a tokamak, nuclear fusion reactor, the divertor is subjected to a high heat flux. Tungsten has been chosen as its plasma facing material and CuCrZr alloy was chosen as the heat sink material. The dissimilarity between both materials: the high ductile-brittle transition temperature of tungsten and the low service temperature of CuCrZr, will lead to a less efficient heat extraction and shorter service life time. In this work, study begins on high-entropy alloy system in an attempt to search for an alternative bond coat material for thermal barriers to smooth the thermal transition.

High entropy alloys are part of a novel area of metallurgy concerning alloys containing at least 5 elements with compositions ranging from 5 at.% to 35 at.%. The interest arises as it has been verified, for plenty compositions, the formation of metastable simple solid solutions with promising properties, pertaining their use in nuclear fusion as thermal barriers, such as high strength and hardness at high temperature, low thermal diffusivity and high radiation resistance.

The CrCuFeMoTi and CrCuFeTiV systems were studied. The compositional effect was identified by producing 6 samples by vacuum arc melting. Three of $CrCu_xFeMoTi$ and three other of $CrCu_xFeTiV$, where x denotes the varying copper molar ratio. The production method was evaluated by producing a single CrCuFeTiV sample by mechanical alloying, for 20 hours at 400 rpm, followed by spark plasma sintering at a pressure of 65 MPa at 900 ºC. The samples were characterized by SEM, XRD and EBSD analysis. The samples produced by arc melting revealed complex multiphasic microstructures, having both systems the same type of Laves matrix phase and other copper and titanium rich phases distributed throughout the matrix. The $CrCu_xFeMoTi$ revealed a heavy segregation of molybdenum, likely related to its higher melting temperature and binary enthalpy of mixing with the other elements. In the $CrCu_xFeTiV$ system a BCC solid solution was identified, yet it did not fully dissolve the remaining elements. The sintered CrCuFeTiV possessed a much simpler structure, with copper rich regions, and an FCC solid solution as the matrix, with another unidentified phase. Argon ions were used to simulate conditions of irradiation in the sample.

Results suggest that control of copper and titanium content are key to obtain solid solutions and that improvement of milling process can enhance the creation of simple structures.

Keywords: high entropy alloy; mechanical alloying; vacuum arc melting; microstructure; irradiation; spark plasma sintering.

Introduction

The work is divided by the production method of the alloys, starting by the vacuum arc melting method, comparing the two systems produced by it. The use of

Experimental methods

The following tables (Table 1 and Table 2) describe molar ratio and atomic percentages of the prepared compositions in the studied HEA systems.

Table 1- Molar ratio and atomic percentage of all the compositions of $CrCu_xFeMoTi$ system

Sample	Cu (at.%)	Cr (at.%)	Fe (at.%)	Mo (at.%)	Ti (at.%)
x=0.21	5	23.75	23.75	23.75	23.75
x=0.44	10	22.5	22.5	22.5	22.5
x=1	20	20	20	20	20

Table 2 - Molar ratio and atomic percentage of all the compositions of $CrCu_xFeTiV$ system

Sample	Cu (at.%)	Cr (at.%)	Fe (at.%)	Ti (at.%)	V (at.%)
x=0.21	5	23.75	23.75	23.75	23.75
x=0.44	10	22.5	22.5	22.5	22.5
x=1	20	20	20	20	20

Pure Cr, Cu, Fe, Mo, Ti and V elements with purity >99 at.% were used for both molten and milled samples. The elements were weighed to obtain samples with compositions described in Table 1 and Table 2. The six compositions were melted in a vacuum arc furnace with a water cooled copper crucible, at least three times to ensure homogeneity before quenching to room temperature. The measured mass loss was less than 1%. For the solid route only one equiatomic sample (x=1) of the CrCuFeTiV system was prepared. The elements were weighted in a glove box in an argon atmosphere. The powder suffered high-energy ball milling in a planetary ball mill, PM 400 MA Type, with stainless steel balls and vials. The ball to powder ratio was 10:1 (6.142g of powder to 63.260g of balls), and a solution of 90% ethanol anhydrous, 5% methanol and 5% isopropanol was used as PCA. The milling occurred for 20 hours at 400 rpm. The MA powders were consolidated by Spark Plasma Sintering, at a pressure of 65.2 MPa at 905ºC with a holding

time of 5 minutes. The process of heating and cooling took 25 minutes overall. Details of the pressure and temperature of the cycle are represented in Figure 1.

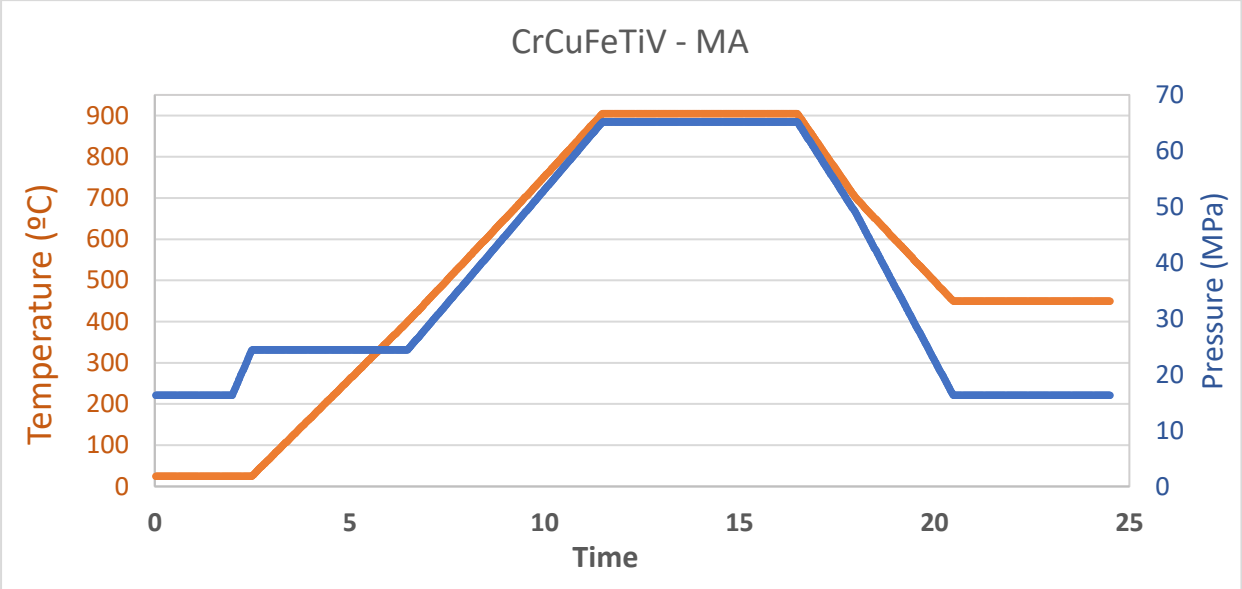

Figure 1 - Sintering curve showing variation of temperature and pressure with time

Implantation was performed aiming to simulating in a few hours the equivalent effect of 5 years of continuous irradiation of neutrons in fusion reactors. According with Baluc et al. [1], damage rate in steels (dpa/year: displacements per atom per year) in first wall condition of fusion reactors, is of 20-30 dpa/year. The equiatomic, sintered CrCuFeTiV-MA sample was submitted for implantation. The irradiation energies and fluences used for the argon ions (Ar^+) were calculated using the SRIM software package [2][3]. To attain the peak damage of 100 dpa (assuming a 20 dpa/year for the estimated operation time of a cassette divertor of 5 years), 300 keV Ar^+ ions to the fluence of $3x10^{16}$ at/cm^2 at room temperature were used. The irradiated sample is denoted as CrCuFeTiV-imp.

Results and discussion

Liquid route

The system revealed multiphasic morphology and the microstructure evolution with increasing copper content is represented in Figure 2. There were 8 identified phases, denoted as **A1**, the grey matrix region; **B1**, brighter regions mainly present at higher copper contents with defined edges; **C1**, is similar and appears next to **B1** but is less light; **D1**, slightly dark regions; **E1**, the darkest regions, appears close to **E1**; **F1** and **G1** always appear tangles in one another, appears on the surface of **H1**, is slightly brighter than **B1** and their edges are smoother; and lastly **H1**, is the large brighter regions.

One of the main evolutions noted as we increase copper content of the samples, is the increase in the volume fraction of dispersed phases, mainly phases **B1**, **C1**, **F1** and **G1**, through the matrix. Also, the change of the morphology of the dispersed phases, from roundish shapes in x=0.21 to directional growth in the other samples.

$CrCu_{0.21}FeMoTi$

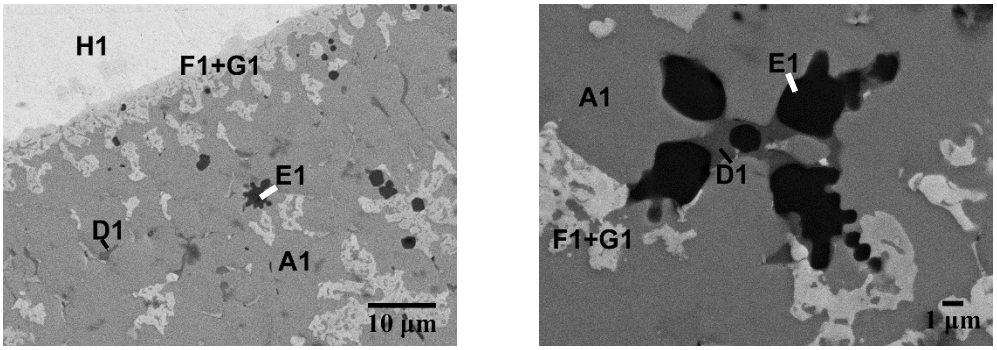

$CrCu_{0.44}FeMoTi$

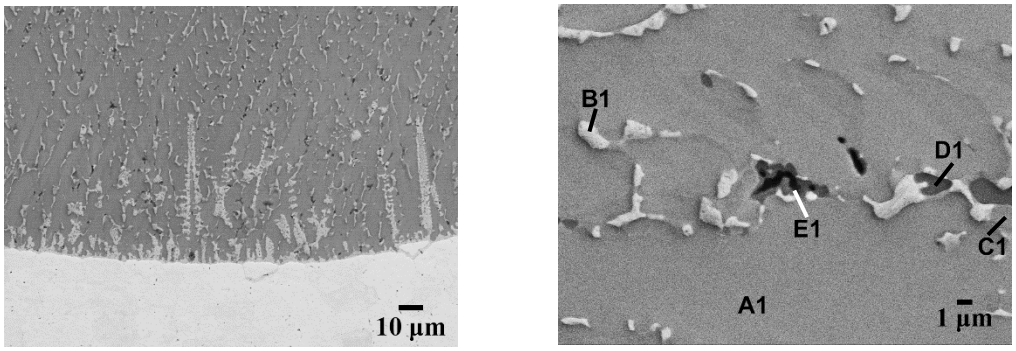

CrCuFeMoTi

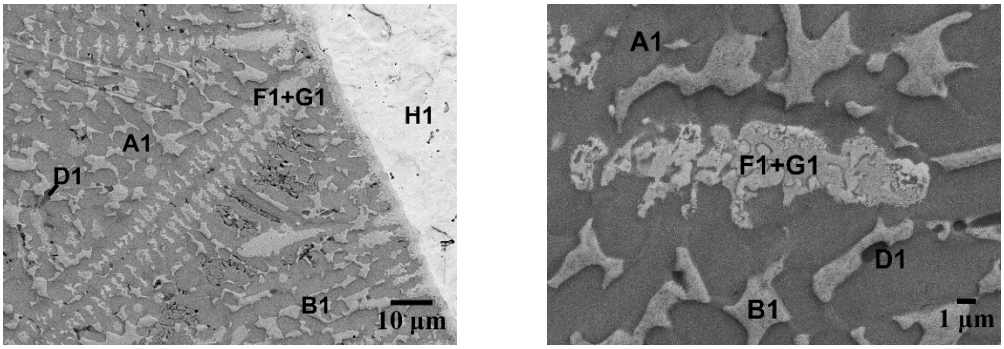

Figure 2 - Microstructures of $CrCu_xFeMoTi$ for x=0.21 for a) and d); x=0.44 for b) and e) and x=1 for c) and f)

Upon exchanging molybdenum for vanadium in the same system, once again we obtain a multiphasic structure. In Figure 4-7 the microstructure of the three sample are represented with BSE images in low magnification and high magnification. There were 5 identified phases: **A2** the grey matrix phase; **B2**, the brighter regions; **C2**, appears close and is similar to **B2** but lees bright; **D2**, is the darker phase seen and **E2**, has dark grey hue and is considered as matrix phase also distributed throughout the sample. The results of the EDS analysis are present in **Error! Reference source not found.**.

Phases **B2**, **C2** and **D2** had a small volume in the x=0.21 and x=0.44 samples, being accurate EDS readings only possible in the equimolar sample where these phases present themselves larger. As seen in Figure 4-7 (f). Another notable phase evolution, is that increased copper content leads to an increase in volume fraction of these phases **B2**, **C2** and **D2**. The addition of copper to the system did not promote the formation of new phases, changing only the fraction of the formed phases.

In composition x=0.21, phase **C2** is noted around phase **E2**, together with small grains of **B2** and **D2**, (Figure 4-7 (a) and (b)), perhaps its nucleation is dependent on phase **E2** or it is indication of the segregation of copper during formation of both phase **A2** and **E2**. As we increase copper content to x=0.44, the three phases increase although, **C2** remains the most relevant of the trio, (Figure 4-7 (c) and (d)), still surrounding phase **E2**. Upon reaching the equimolar composition, phase **B2** becomes the most relevant of the three, besides appearing to no longer need to surround phase **E2**. Indicating that these three phases are related through a reaction.

Two phases coexist as the matrix of the sample, labeled phases **A2** and **E2**. As the volume of the previous three described phases increases, these two major phases become less interconnected, going from a practically continuous phase **A2**, Figure 4-7 (a), to a discontinued phase, Figure 4-7 (f).

Supporting EDS results (**Error! Reference source not found.**) and an x-ray map (**Error! Reference source not found.**) were obtained, here we clearly see the distribution of the elements in the equimolar sample, which contains the larger volume fraction of each phase.

$CrCu_{0.21}FeMoTi$

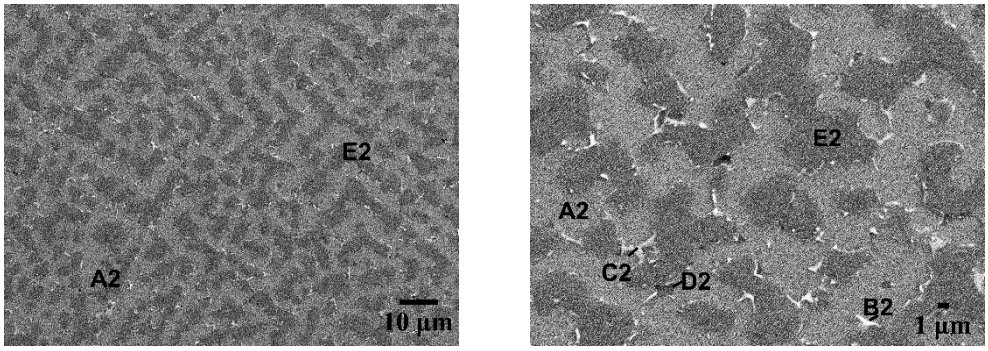

$CrCu_{0.44}FeMoTi$

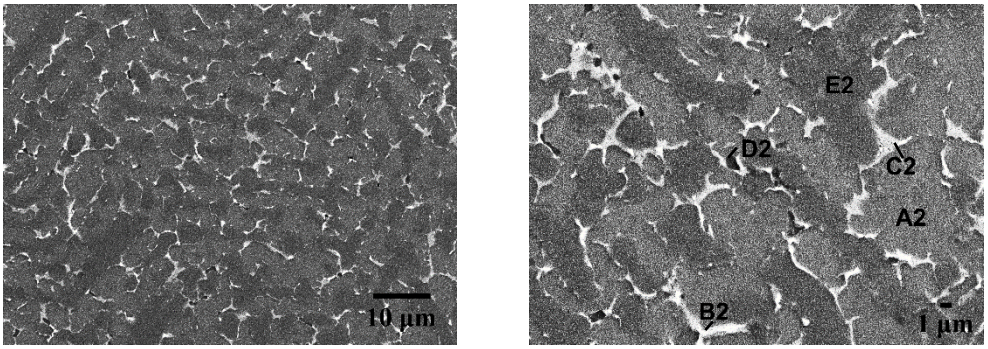

CrCuFeMoTi

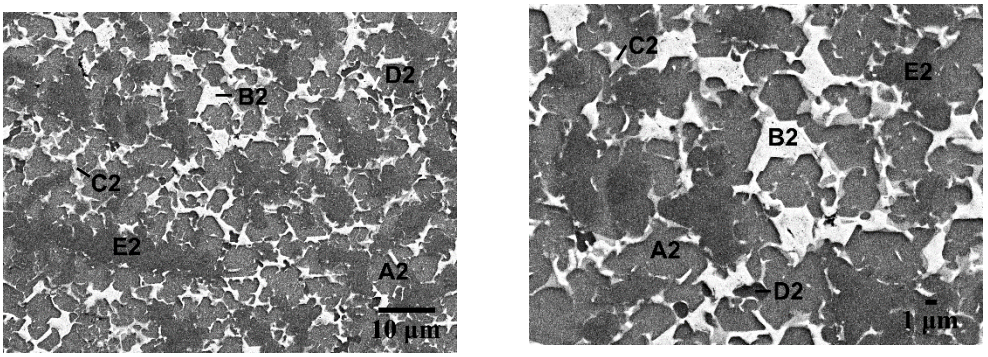

*Figure **Error! No text of specified style in document.**-3 - BSE/SEM images showing the microstructure of CrCuxFeTiV with a) and b) x=0.21, c) and d) x=0.44, e) and f) x=1*

Solid route

Secondary electron images of the microstructure of the as-sintered sample are evidenced in Figure 5-1. The sample has very fine microstructure, phases being around 1µm in size, indicating sub micrometric grain size. Three phases can be identified, noted as **A**, **B**, and **C** in Figure 5-1, and the corresponding EDS analysis is presented in **Error! Reference source not found.**.

According to EDS point analysis, region **A** is a copper rich phase. Phase **B** is depleted in copper but is richer in chromium and poorer in titanium. The latter phase **C** is distributed throughout the whole sample, it has less copper content and an approximate similar distribution of the remaining element in the composition.

Throughout the sample small black spots are observed. These denote nanoporosity, confirmed by the SE images of the sample tilted at 70º in Figure 5-2. This porosity is a lot less prevalent in phase A and B, but is more common throughout the matrix phase C.

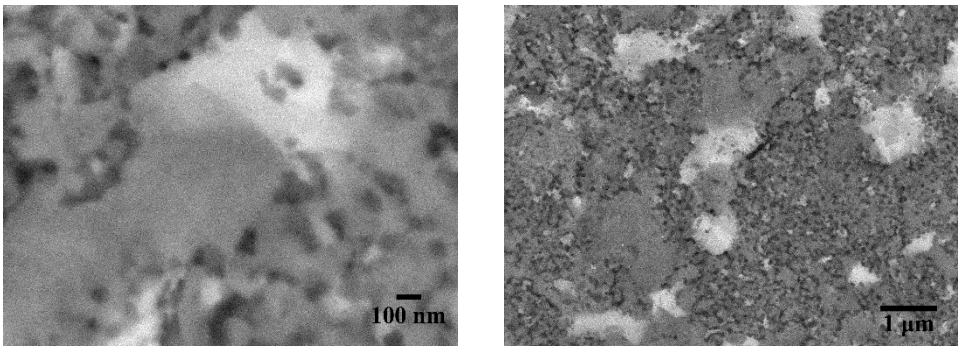

Figure **Error! No text of specified style in document.**-4 - SE micrographs of the surface of the consolidated sample

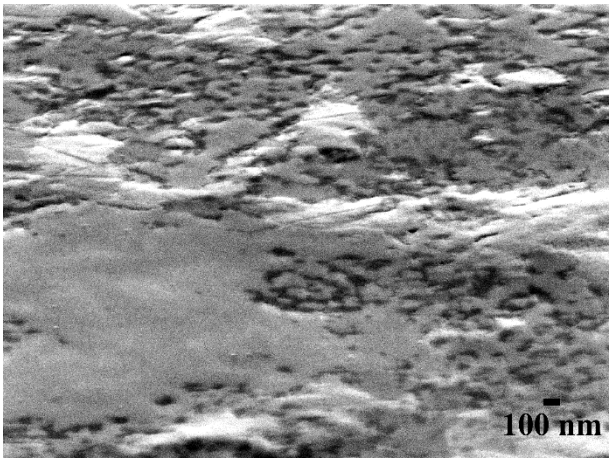

Figure **Error! No text of specified style in document.**-5 - SE micrograph tilted at 70º revealing detail of porosity

The only noted changes in the microstructure was the formation of craters, due to the sputtering effect of the argon ions, Figure 5-7. The fact that no blistering, swelling or fissuration is observed, may indicate low retention of the ions and no loss of ductility of the material.

The diffractograms from both as-sintered and implanted samples are represented in **Error! Reference source not found.**. The as-sintered sample reveals clean peaks with very low noise whereas the implanted sample has a lower signal-to-noise ratio, this is probably due to the disorder induced in the structure by the collision of the ions. It is possible for metals to become amorphous when subjected to ion beams, if the free energy of the crystal increases due to the increase of radiation induced defects[4] and the greater atomic strains in concentrated solutions in HEA can lead to amorphization by irradiation easier[5]. The GXRD does not reveal full amorphization but indicates that there has been some structural disorder induced during implantation.

It seems that the heavy argon ions induced a massive massive phase transformation observed from FCC to BCC. Although nanomaterials do possess large defect sinks (high density of grain boundaries) where interstitials and vacancies can anhilate, the multicomponent crystal may not allow elimination of such defects leading to the crystalline structure to change to a BCC phase. This phase transformation, may indicate that the original major FCC1 phase was heavily strained from the MA, and the SPS was able to maintain this out of equilibrium phase. Upon implantation, sufficient energy was given to the atoms to move to more relaxed position, originating a BCC structure with a much more open structure. Moreover, according with the used elements and the valence electron concentration a BCC structure would be expected and the ion beam just allowed a more stable state to be reached.

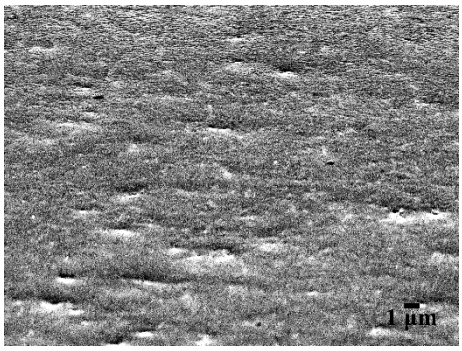

*Figure **Error! No text of specified style in document.**-6 - 70º tilted image of implanted sample. The sulks observed are craters resulting from the implantation*

Conclusions

The increase in copper content in the vacuum arc melting samples did not lead to its dissolution within the formed phases, instead it increases the volume fraction of copper rich structures in both the systems. The formation of these copper rich structures is associated to the high binary enthalpy of mixture of copper with the remaining metals. This promotes phase separation and decreases likelihood of formation of single phases. Both systems contained as the matrix phase an ordered C14 laves phase because of the interaction of titanium with the other elements.

Segregation of Molybdenum occurred in all three samples of $CrCu_xFeMoTi$, leading to a depletion of Mo in the melt and by consequence the formed structures. On the other hand the $CrCu_xFeTiV$ system had no large segregation of species but the matrix phase was separated between an ordered laves phase and BCC solid solution.

The expected entropy effect was not verified for these systems as the metastable solid solutions did not dominate over the remaining phases. It is proposed that a reduction of the atomic ratio of both copper and titanium, could promote simpler structures, by preventing phase separation of copper rich phases and reducing the tendency of ordering the laves phase structure. In the case of the mechanically alloyed sample, increase of milling time could “force” the dissolution of remaining copper.

References

[1] N. Baluc *et al.*, “Status of R&D activities on materials for fusion power reactors,” *Nucl. Fusion*, vol. 47, no. 10, pp. S696–S717, 2007.

[2] http://www.srim.org, “SRIM 2013 Software Package.” .

[3] J. F. Ziegler, M. D. Ziegler, and J. P. Biersack, “SRIM - The stopping and range of ions in matter (2010),” *Nucl. Instruments Methods Phys. Res. Sect. B Beam Interact. with Mater. Atoms*, vol. 268, no. 11–12, pp. 1818–1823, 2010.

[4] N. Karpe, K. K. Larsen, and J. Bo/ttiger, “Phase formation induced by ion irradiation and electrical resistivity of aluminum–3 d -transition-metal alloys,” *Phys. Rev. B*, vol. 46, no. 5, pp. 2686–2692, Aug. 1992.

[5] T. Egami, M. Ojha, O. Khorgolkhuu, D. M. Nicholson, and G. M. Stocks, “Local Electronic Effects and Irradiation Resistance in High-Entropy Alloys,” *Jom*, vol. 67, no. 10, pp. 2345–2349, 2015.